

Pluvials, droughts, the Mongol Empire, and modern Mongolia

Neil Pederson^{a,1,2}, Amy E. Hessl^{b,1,2}, Nachin Baatarbileg^c, Kevin J. Anchukaitis^d, and Nicola Di Cosmo^e

^aTree Ring Laboratory, Lamont-Doherty Earth Observatory, Columbia University, Palisades, NY 10964; ^bDepartment of Geology and Geography, West Virginia University, Morgantown, WV 26506; ^cDepartment of Forestry, National University of Mongolia, Ulaanbaatar, Mongolia 14201; ^dDepartment of Geology and Geophysics, Woods Hole Oceanographic Institution, Woods Hole, MA 02543; and ^eSchool of Historical Studies, Institute for Advanced Study, Princeton, NJ 08540

Edited by Karl W. Butzer, The University of Texas at Austin, Austin, Texas, and approved February 11, 2014 (received for review October 2, 2013)

Although many studies have associated the demise of complex societies with deteriorating climate, few have investigated the connection between an ameliorating environment, surplus resources, energy, and the rise of empires. The 13th-century Mongol Empire was the largest contiguous land empire in world history. Although drought has been proposed as one factor that spurred these conquests, no high-resolution moisture data are available during the rapid development of the Mongol Empire. Here we present a 1,112-y tree-ring reconstruction of warm-season water balance derived from Siberian pine (*Pinus sibirica*) trees in central Mongolia. Our reconstruction accounts for 56% of the variability in the regional water balance and is significantly correlated with steppe productivity across central Mongolia. In combination with a gridded temperature reconstruction, our results indicate that the regional climate during the conquests of Chinggis Khan's (Genghis Khan's) 13th-century Mongol Empire was warm and persistently wet. This period, characterized by 15 consecutive years of above-average moisture in central Mongolia and coinciding with the rise of Chinggis Khan, is unprecedented over the last 1,112 y. We propose that these climate conditions promoted high grassland productivity and favored the formation of Mongol political and military power. Tree-ring and meteorological data also suggest that the early 21st-century drought in central Mongolia was the hottest drought in the last 1,112 y, consistent with projections of warming over Inner Asia. Future warming may overwhelm increases in precipitation leading to similar heat droughts, with potentially severe consequences for modern Mongolia.

paleoclimate | dendrochronology | human ecology | Anthropocene | coupled human natural systems

Abrupt climate changes have immediate and long-lasting consequences for ecosystems and societies. Although studies have linked the demise of complex societies with deteriorating climate conditions (1–4), few, if any, have investigated the connection between climate, surplus resources, energy, and the rise of empires. The rapid expansion of the Mongols under Chinggis Khan (also known as Genghis Khan) from 1206 to 1227 CE resulted in the largest contiguous land empire in world history (Fig. 1, inset). The Mongol conquests affected the history of civilizations from China to Russia, Persia to India, and even left a genetic fingerprint on the people of Eurasia (5). Although historians have proposed climate as a possible factor in Mongol history (6), few paleoenvironmental data of the necessary temporal resolution are available to evaluate the role of climate, grassland productivity, and energy in the rise of the 13th-century Mongol Empire.

Lake sediment data from central Mongolia suggest that the climate of the Mongol Empire may have been unusually wet (7), but the temporal resolution of these records is too coarse to capture conditions during the 2 decades of rapid growth of the Mongol Empire. Annual tree-ring records of past temperature from central Mongolia extending back to 558 CE document warm conditions during the 11th century, consistent with other Northern Hemisphere records, but also indicate a subsequent

warm period during the 12th and 13th centuries (8, 9). Millennium-long reconstructions of past precipitation in western China, mostly located on the Tibetan Plateau and north central China (10–15), document drought during the early 1200s. However, periods of drought in central Mongolia are generally out of phase with drought on the Tibetan Plateau (2), and there is little reason to believe that moisture conditions on the Tibetan Plateau and north central China would be consistent with that of central Mongolia. Here we present the first, to our knowledge, annually resolved record of moisture balance covering the last millennium in High Asia. This new record allows us to evaluate the hypothesis that drought drove the 13th-century Mongol expansion into Eurasia (6, 16).

Results

We present a 1,112-y tree-ring reconstruction of warm-season, self-calibrating Palmer Drought Severity Index (scPDSI) (17) (*Supporting Information*), a measure of aggregate water balance, derived from 107 living and dead Siberian pine (*Pinus sibirica*) trees growing on a Holocene lava flow in central Mongolia (Fig. 2). Trees growing on the Khorgo lava flow today are stunted and widely spaced, occurring at the lower tree line on microsites with little to no soil development. These trees are severely water-stressed, and their radial growth is well correlated with both moisture availability (scPDSI) and grassland productivity [Normalized Difference Vegetation Index (NDVI)] (Fig. 3). Our reconstruction, calibrated and validated on instrumental June–September scPDSI (1959–2009) (*Table S1*), accounts for 56% of the variability in the

Significance

A 1,112-y tree-ring record of moisture shows that in opposition to conventional wisdom, the climate during the rise of the 13th-century Mongol Empire was a period of persistent moisture, unprecedented in the last 1,000 y. This 15-y episode of persistent moisture likely led to a period of high grassland productivity, contributing fuel to the Mongol Empire. We also present evidence that anthropogenic warming exacerbated the 21st-century drought in central Mongolia. These results indicate that ecosystems and societies in semiarid regions can be significantly affected by unusual climatic events at the decadal time scale.

Author contributions: N.P. and A.E.H. designed research; N.P., A.E.H., and N.D.C. performed research; N.P., A.E.H., and K.J.A. analyzed data; and N.P., A.E.H., N.B., K.J.A., and N.D.C. wrote the paper.

The authors declare no conflict of interest.

This article is a PNAS Direct Submission.

Data deposition: All tree ring data have been deposited in the International Tree Ring Databank, www.ncdc.noaa.gov/paleo/treering.html.

¹N.P. and A.E.H. contributed equally to this work.

²To whom correspondence may be addressed. E-mail: adk@ldeo.columbia.edu or Amy.Hessl@mail.wvu.edu.

This article contains supporting information online at www.pnas.org/lookup/suppl/doi:10.1073/pnas.1318677111/-DCSupplemental.

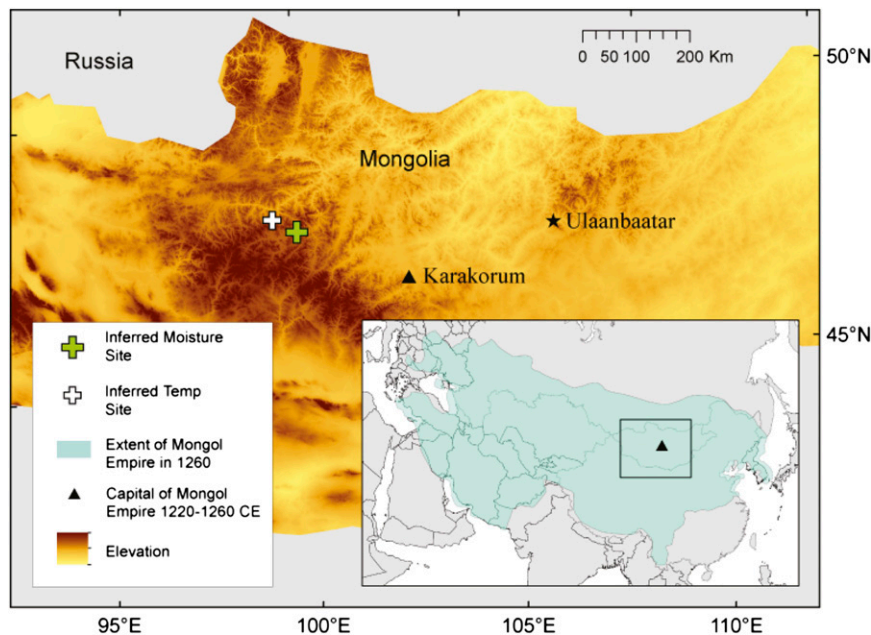


Fig. 1. Tree-ring drought reconstruction site (green cross) and inferred temperature site (8) (white cross) are 50 km apart. Map of the Mongol Empire near its zenith (aqua) in 1260 CE (inset). The ancient capital city of Karakorum (black triangle) and current capital of Mongolia, Ulaanbaatar (black star).

regional scPDSI (17) during the months when 73% of the annual rainfall occurs.

Our reconstruction covers important climatic eras of the last millennium including the Medieval Climate Anomaly (MCA), the Little Ice Age, and the beginning of the Anthropocene (Fig. 2). The MCA was characterized by several severe and persistent droughts in central Mongolia. The first half of the 900s was generally dry with an extended drought between 900 and 964 CE. Similarly, 1115–1139 CE and 1180–1190 CE were extremely dry, with periods of below-average reconstructed scPDSI. The 1180s drought occurred during the turbulent early years of Chinggis Khaan, a historical period characterized by warring tribes and factions on the Mongolian steppe (18). These droughts were followed by a wet period beginning in the early 13th century and then a return to drier conditions until the late 14th century. From there, multiannual to decadal-scale variation in hydroclimate continued until the 20th century when climate was wetter than any other century since 900 CE.

The most unusual period in the 1,112-y record was not marked by extreme variability but was instead persistently wet. From 1211 to 1225 CE, no annual values or their bootstrapped confidence limits drop below the long-term mean of the reconstruction, making it an unmatched “pluvial,” a prolonged period of above-average moisture, over the last 1,112 y (Figs. 2A and B and 4A and B). Although individual years (e.g., 1959 and 1993) and other centuries (e.g., 20th century) were wetter, the mean of this 15-y pluvial (0.600 ± 0.589) was nearly 1 SD above the long-term mean of the reconstruction (-0.546 ± 1.550). This consistently wet period with low variance ended with a 4-y drought beginning in 1226 CE, followed by a return to high moisture variability characteristic of much of the last millennium. In addition to being wet, early 13th-century central Mongolia was warm (Fig. 4A and Fig. S1). Reconstructed temperature anomalies over extratropical Asia from 1211 to 1225 CE were warm (-0.118 ± 0.147 °C) and above the long-term (900–2009 CE) mean (-0.311 ± 0.292 °C) but were not exceptionally hot (Fig. S2). These data indicate that the expansion of the Mongols under Chinggis Khan occurred in a consistently wet and warm environment not witnessed during any other time in the last 1,112 y.

Discussion

Most energy exploited by human societies in 13th-century Mongolia was derived from the productivity of grasslands. Herbivores, be they domesticated or wild, are closely tied to climatic conditions via net primary productivity (19, 20), and net primary productivity of Mongolia’s steppe is directly linked to growing season moisture availability (21). This relationship is reflected in the strong positive correlation between our tree-ring chronology and NDVI of the central Mongolian steppe (Fig. 3B). The warm and consistently wet conditions of the early 13th century would have led to high grassland productivity and allowed for increases in domesticated livestock, including horses.

Dry climatic conditions from the 1180s to the early 13th century coincided with extreme political instability in Mongolia, characterized by continuous warfare, the deterioration of established hierarchies, and a remaking of the political order that accompanied the rise of Chinggis Khan (22–24). Although the historical reasons for the worsening of the relations among the aristocratic groups ruling Mongolia have been attributed to social and political events, based on the biography of Chinggis Khan (23, 24), actual historical evidence is extremely scarce. Regardless of the causes that set in motion initial conflicts, it can be surmised that the worsening dry conditions reconstructed for the end of the 12th century would have been an important contributing factor in the collapse of the established order and emergence of a centralized leadership under Chinggis Khan. What might have been a relatively minor crisis instead developed into decades of warfare and eventually produced a major transformation of Mongol politics.

Our paleoclimate data show a dramatic change in temperature and precipitation in the 13th century that would have translated into enhanced productivity and increased availability of energy in the steppes, specifically in the Orkhon Valley region. Climatic variability, hypothetically, could have provided ample resources for strengthening the new unified leadership. As we know from historical sources, both the army and government were entirely reconstituted under Chinggis Khan, and such a strong and unified center would have required a concentration of resources that only higher productivity could have sustained in a land in

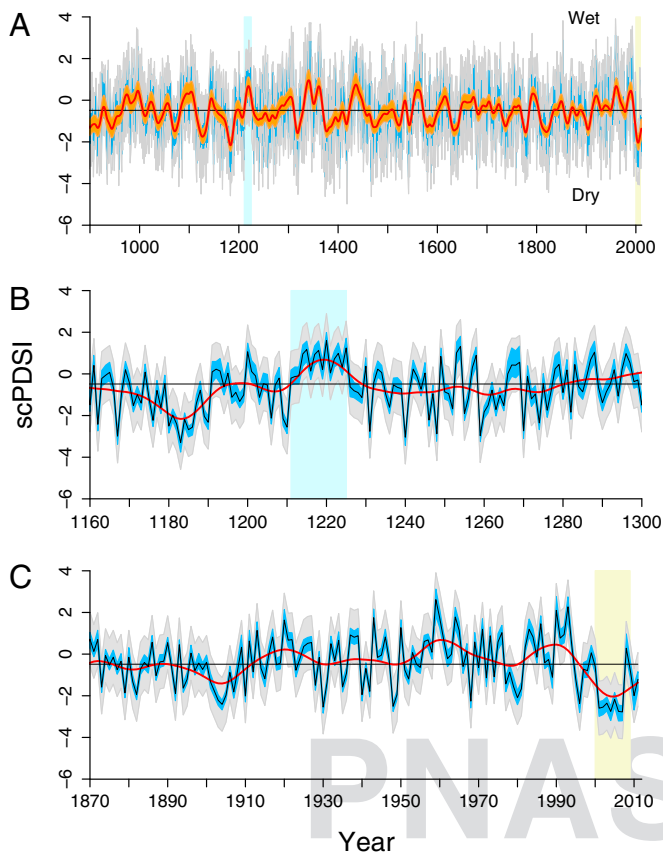


Fig. 2. Reconstructed drought from (A) 900–2011 CE, (B) 1160–1300 CE, and (C) 1870–2011 CE. Moisture balance highlights include the extended 15-y Mongol Pluvial (1211–1225 CE; blue box) and 21st-century drought (yellow box). A shows 20-y spline of the annual reconstruction (red). Two-tailed 95% bootstrap confidence limits of the reconstruction (blue) and spline (orange) were scaled to the reconstructed scPDSI. The uncertainty of the reconstruction is shown in gray (± 1 RMSE). The severe drought during the 1180s, the Mongol Pluvial (blue bar), and the significant drought during the movement of the empire capitol to China in 1260 CE are presented in B. The multiple pluvial events during the 20th century and the reversal to the severe and extended 21st-century drought (yellow bar) are highlighted in C. Annual values (black) are plotted in B and C.

which extensive pastoral production does not normally provide surplus resources.

The increased carrying capacity of the land might explain the movement of the center of the Mongol Empire to the Orkhon Valley from the Onon River region, where Chinggis was elevated to the rank of Great Khan and had his power base. During Chinggis's lifetime, the Orkhon Valley became a center of military operations, and according to Chinese sources, Chinggis Khan established the capital there in 1220 (25). It is likely that this was only a supplementary area of military operations and the site of Ögödei Khan's (Chinggis Khan's third son and successor, r. 1229–1241) power because the center of the empire remained in the Onon–Kerülen area. However, historical records show across Mongolia the formation of large imperial camps (*ordu*) of hundreds of and perhaps thousands of car tents (26).

The transfer of the political center of the empire to Karakorum in the later part of Chinggis's life and, especially as the capital of the Mongol Empire under Ögödei Khan, would support the hypothesis that the greater productivity of the steppes favored larger concentrations of peoples, armies, and courts. Wet and warm conditions enabled the Mongol leadership to concentrate political and military power in designated localities.

It is this condition that was a necessary and important factor in the successful mobilization of nomadic power in Chinggis Khan's military expeditions.

Although some historians have considered a deteriorating climate as a possible factor that explained the initial drive of the Mongols against their sedentary neighbors (6), our tree-ring evidence now shows that rapid expansion of the Mongols after their unification is correlated with favorable climate conditions, which were conducive not just to increased pastoral production but to the political centralization and military mobilization that would make conquest possible. The successful campaigns of the Mongols between 1206 and 1225 against the Tangut, Jurchen, and central Asian regimes enabled the construction of a solid and sophisticated politico-military state, which in a more advanced state of the conquest could support itself not just with local resources but also with the exploitation of conquered regions (18).

Our 1,112-y drought-sensitive chronology also provides a longer context for the climatic changes observed during the 20th and 21st centuries, another period of rapid economic and cultural transformation in Mongolia. During the 20th century, regional climate was wetter than any of the previous 11 centuries, with 9 decades above the long-term mean. These wet conditions occurred during a period of widespread agricultural development (27). The unusually wet decades of the last half of the 20th century (Fig. 4A) were followed by a severe drought and three *dzuds* (a combination of severe climatic conditions that results in

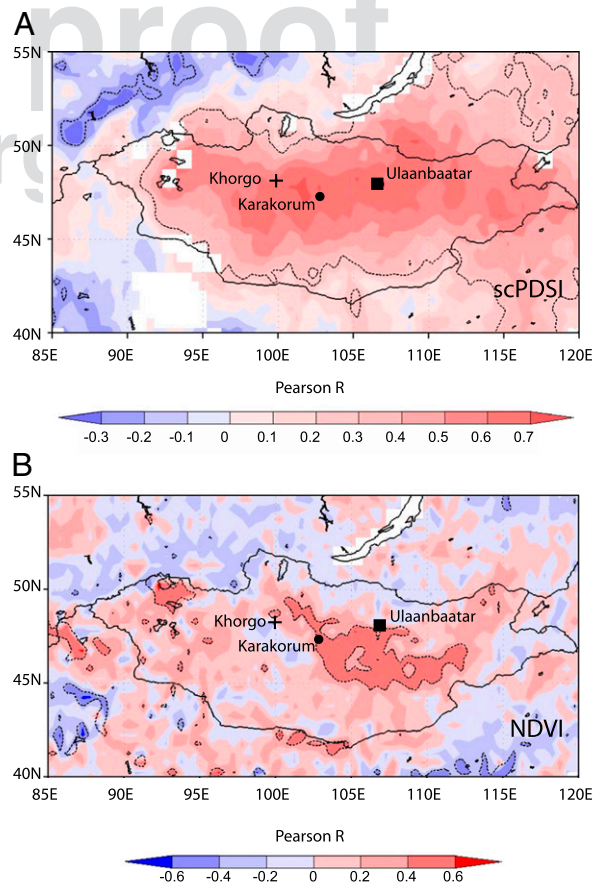


Fig. 3. (A) Correlation with mean June–September scPDSI (17), a measure of water balance, and (B) correlation with Global Inventory Modeling and Mapping Studies NDVI (1980–2010) (31), a satellite-derived measure of grassland productivity, lagged 1 y forward. Shown are 95% CIs (dashed lines), tree-ring chronology (cross), ancient capital of Mongol Empire Karakorum (small circle), and Ulaanbaatar (square).

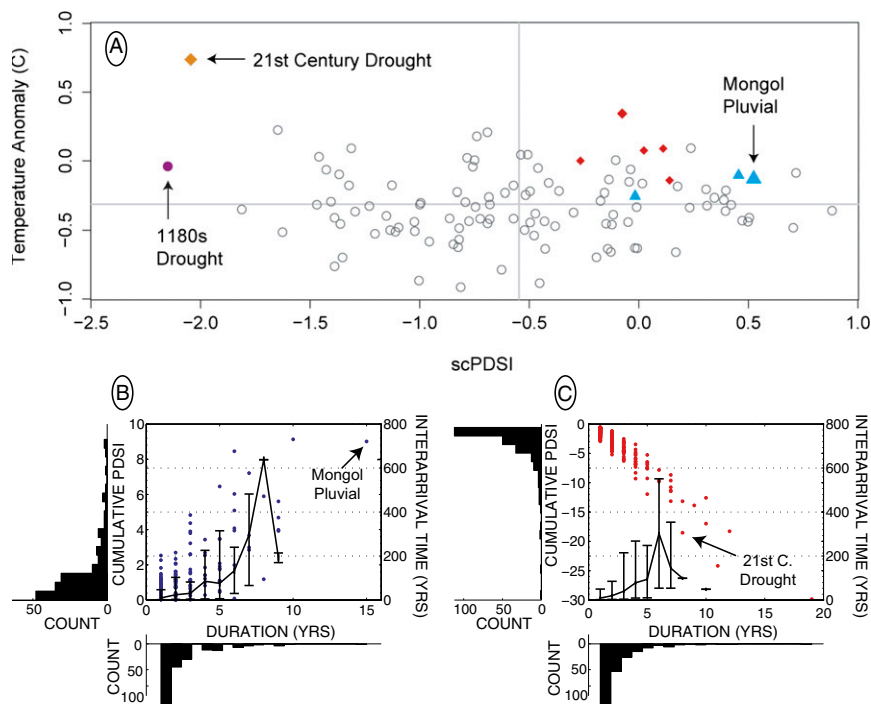


Fig. 4. Decadal means of reconstructed temperature over extratropical Asia (32) versus reconstructed scPDSI (17) from 900 to 2009 CE (A). The exception to the decadal mean data is the large blue triangle representing the average for the 15-y Mongol Pluvial during the expansion of the 13th-century Mongol Empire (1211–1225 CE). Highlighted decades within this plot include the 2 decades during the Mongol Pluvial (1210–1219 CE and 1220–1229 CE; small blue triangles), the 1180–1189 CE drought (purple dot), the last 5 decades of the 20th century (1950–1999; red diamonds), and the 21st-century drought (2000–2009) (orange diamond). Cumulative scPDSI versus duration of pluvial events (B) and droughts (C) demonstrates that the Mongol Pluvial was an exceptionally sustained period of moisture and the 21st-century drought was the third most severe drought in the last 1,112 y following only the 1120s and 1180s drought events, which occurred in a cooler climate.

high mortality of livestock) between 1998 and 2010. The transition to a market economy during the 1990s stimulated rapid expansion of the nation's livestock populations (28). However, the combination of ensuing drought and *dzud* in the early 21st century appears to have rapidly reduced the carrying capacity generated during the prior period of historically high animal density. For example, as a consequence of the 1999–2002 *dzud*, ~10–20 million livestock were killed, which in turn caused a migration of roughly 180,000 people to the capital city of Ulaanbaatar (28). Our tree-ring reconstruction of scPDSI suggests that the severity of the 21st-century drought was matched only by the 1180s droughts (Fig. 4C), which occurred during a substantially cooler climate (Fig. 4A and Fig. S1). Average instrumental June–September temperatures during the 21st-century drought (2000–2009) were ~1.9 °C warmer than the mean of the 20th-century record (1959–1999). Reconstructed temperatures during the 21st century were >3.5 SD higher than the reconstructed mean from 900 to 2009 over extratropical Asia (21st-century mean = 0.74 °C; 900–2009 mean = -0.31 °C, SD = 0.29 °C). When our millennial-length chronology of drought is combined with a Mongolian tree-ring temperature reconstruction (Fig. S2C), Asian temperature reconstruction (Fig. S2B), and gridded instrumental climate record (Figs. S2A and S3), the importance of elevated temperature in exacerbating the 21st-century drought is clear.

Unusual decadal-scale events in Mongolia like the Mongol Pluvial and the 21st-century drought had far-reaching social consequences including rapid urbanization and widespread social change. Temperatures in continental central Asia are projected to rise substantially more than the global mean in future decades (29). If future warming overwhelms increased precipitation, episodic heat droughts and their social, economic, and political

consequences will likely become more common in Mongolia and Inner Asia.

Materials and Methods

Tree-Ring Data Collection and Standardization. We collected Siberian pine increment cores and cross-sections throughout the Khorgo lava field in 2010 and 2012 (Table S1) from living and dead trees on thin or absent soils surrounded by dark basalt. We measured total ring width to ± 0.001 mm and cross-dated samples using standard procedures. Our chronology, based on 107 samples, maintains a minimum sample depth of 25 series between 900 and 2009 CE, dropping to 12 in 2010–2011 CE.

We experimented with a variety of standardization techniques to assess the effect of standardization on the reconstruction. Strip-bark, caused by cambial dieback, may enhance decadal to centennial variation in tree-ring records as strip-bark trees allocate more carbon to cambial growth than non strip-bark trees (30), particularly during recovery from dieback. At least 44% of our samples were from strip-bark trees that tended to have more positive growth trends than samples from trees with a complete cambial band. This pattern of increasing growth with age among strip-bark trees is present in the regional growth curve of our strip-bark versus non strip-bark samples (Fig. S4 A and B). For this reason, we detrended the raw tree-ring measurement series using either a negative exponential curve or straight line with slope ≤ 0 (typically samples containing or close to pith), straight line with slope ≤ 0 (typically non strip-bark samples without early growth), or straight line with slope > 0 (typically strip-bark samples). We then compared independent chronologies of strip-bark versus non strip-bark (with pith) and observe minor and insignificant differences in the two chronologies (Fig. S5). The strip-bark chronology has higher overall interannual variance but still maintains the character of the Mongol Pluvial in the early 13th century and the 21st-century drought. Median series length is 472 y (range 252–1,193 y), and the record appears to maintain some variation at centennial time scales. Tests using different standardization methods, including regional curve standardization and signal-free standardization, do not alter our main climatic conclusions: the Mongol Pluvial and 21st-century drought are present and unusual regardless of methodology.

Climate Data. Mongolia's climate stations are sparse and at times incomplete, particularly since 1980. For example, two stations near our study site with >60 y of data (Muren and Uliastai) contain 12–15% missing monthly values since 1980. We instead chose to use the gridded scPDSI derived from Climatic Research Unit 3.20 precipitation and potential evapotranspiration fields (17) (*scPDSI*). With these gridded data, our reconstruction accounts for slightly under 56% of the variance in the observational scPDSI (actually, $r^2 = 55.8\%$). Uncertainty in the reconstruction may arise in part due to the sparse and heterogeneous climate data.

scPDSI. scPDSI (17) is a modified version of PDSI that addresses some of the major limitations of PDSI. scPDSI uses the physically based Penman–Monteith equation for potential evapotranspiration rather than Thornthwaite function used in PDSI. The Penman–Monteith equation incorporates daily temperature, radiation, wind speed, and humidity, whereas the Thornthwaite function uses only temperature and day length. Further, scPDSI applies actual vegetation cover rather than a reference crop, as in the original PDSI. scPDSI is also corrected for seasonal snowpack dynamics and has a similar range of variability in diverse climates, allowing different regions to be compared.

Tree-Ring Reconstruction of scPDSI. The average correlation between tree-ring series (\bar{r}) in our chronology is 0.728 (SD = 0.044), indicating that tree growth is responding to a common environmental signal (Fig. S6). The average expressed population signal, a metric that quantifies how well a chronology based on a finite number of trees represents a hypothetical perfect or true

chronology, is 0.990 (possible range 0–1.0), indicating adequate sample size from 900 to 2011. Significant ($P < 0.05$) correlations with current growing season local meteorological station precipitation data (Pearson correlation coefficient, $r = 0.49$), Selenge River streamflow ($r = 0.57$), and temperature ($r = -0.54$) indicate that radial growth of these trees is primarily limited by soil moisture. Spatial correlations with gridded observational scPDSI are spatially coherent and cover most of Mongolia and High Asia (Fig. 3A).

Calibration/Validation. We reconstructed average June–September scPDSI for central Mongolia (48–52°N, 88–120°E) using a linear regression model relating June–September scPDSI to our ring width chronology using all data from 1959 to 2009 (Fig. S7). We then validated our model and estimated prediction error using a split-period cross-validation approach by partitioning our time series into two 25-y periods (1959–1984 and 1985–2009) (Table S1).

ACKNOWLEDGMENTS. We are grateful for the support of field and laboratory technicians: John Burkhart, Oyunsanaa Byambasuren, Shawn Cockrell, Kristin DeGrauw, Joseph James, Caroline Leland, Dario Martin-Benito, Javier Martin-Fernandez, Byarbaatar Soronzonbold, and Balginnyam Ulziibayar. We thank Gerard van der Schrier for access to scPDSI data. We appreciate comments on the manuscript by Ed Cook, David Frank, Caroline Leland, and Jaime Toro. This research was made possible through grants from National Geographic (9114-12), National Science Foundation (CNH 1210360 and DEB-0816700), West Virginia University Faculty Senate, and The Climate Center of Lamont-Doherty Earth Observatory. This is Lamont-Doherty Earth Observatory Contribution 7759.

- Buckley BM, et al. (2010) Climate as a contributing factor in the demise of Angkor, Cambodia. *Proc Natl Acad Sci USA* 107(15):6748–6752.
- Cook ER, et al. (2010) Asian monsoon failure and megadrought during the last millennium. *Science* 328(5977):486–489.
- deMenocal PB (2001) Cultural responses to climate change during the late Holocene. *Science* 292(5517):667–673.
- Weiss H, et al. (1993) The genesis and collapse of third millennium north mesopotamian civilization. *Science* 261(5124):995–1004.
- Zerjal T, et al. (2003) The genetic legacy of the Mongols. *Am J Hum Genet* 72(3):717–721.
- Jenkins G (1974) A note on climatic cycles and the rise of Chinggis Khan. *Cent Asiat J* 18(18):217–226.
- Shinneman ALC, Almendinger JE, Umbanhowar CE, Edlund MB, Nergui S (2009) Paleolimnologic evidence for recent eutrophication in the Valley of the Great Lakes (Mongolia). *Ecosystems* 12(6):944–960.
- D'Arrigo RD, et al. (2001) 1738 years of Mongolian temperature variability inferred from a tree-ring width chronology of Siberian pine. *Geophys Res Lett* 28(3):543–546.
- Jacoby GC, D'Arrigo RD, Davaajamts T (1996) Mongolian tree rings and 20th century warming. *Science* 273(5276):771–773.
- Holmes J, Cook E, Yang B (2009) Climate change over the past 2000 years in western China. *Quat Int* 194(1–2):91–107.
- Sheppard PR, et al. (2004) Annual precipitation since 515 BC reconstructed from living and fossil juniper growth of northeastern Qinghai Province, China. *Clim Dyn* 23(7–8):869–881.
- Shao X, et al. (2010) Climatic implications of a 3585-year tree-ring width chronology from the northeastern Qinghai-Tibetan Plateau. *Quat Sci Rev* 29(17–18):2111–2122.
- Zhang Q-B, Cheng G, Yao T, Kang X, Huang J (2003) A 2,326-year tree-ring record of climate variability on the northeastern Qinghai-Tibetan Plateau. *Geophys Res Lett* 30(14):1739.
- Liu Y, et al. (2009) Annual temperatures during the last 2485 years in the mid-eastern Tibetan Plateau inferred from tree rings. *Sci China Ser Earth Sci* 52(3):348–359.
- Gong G, Hameed S (1991) The variation of moisture conditions in China during the last 2000 years. *Int J Climatol* 11(3):271–283.
- Fletcher J (1986) The Mongols: Ecological and social perspectives. *Harv J Asiat Stud* 46(1):11–50.
- Van der Schrier G, Barichivich J, Briffa KR, Jones PD (2013) A scPDSI-based global dataset of dry and wet spells for 1901–2009. *J Geophys Res Atmospheres* 118(10):4025–4048.
- Di Cosmo N (1999) State formation and periodization in Inner Asian History. *J World Hist* 10(1):1–40.
- McNaughton SJ, Oesterheld M, Frank DA, Williams KJ (1989) Ecosystem-level patterns of primary productivity and herbivory in terrestrial habitats. *Nature* 341(6238):142–144.
- Fritz H, Duncan RP (1993) Large herbivores in rangelands. *Nature* 364(6435):292–293.
- Ren W, et al. (2007) Influence of ozone pollution and climate variability on net primary productivity and carbon storage in China's grassland ecosystems from 1961 to 2000. *Environ Pollut* 149(3):327–335.
- May TM (2012) *The Mongol Conquests in World History* (Reaktion Books, London).
- Biran M (2007) *Chinggis Khan* (Oneworld, Oxford).
- Masuya T (2013) Seasonal capitals with permanent buildings in the Mongol empire. *Turko-Mongol Rulers, Cities and City Life*, ed Durand-Guedy D (Brill, Leiden, The Netherlands), pp 224–235.
- Cleaves FW (1952) The Sino-Mongolian Inscription of 1346. *Harv J Asiat Stud* 15(1/2):1–123.
- Allsen T (1994) The rise of the Mongolian empire and Mongolian rule in north China. *Alien Regimes and Border States, 907–1368*, Cambridge History of China, eds Franke H, Twitchett D (Cambridge Univ Press, Cambridge, UK), Vol 6, pp 333–348.
- Pederson N, et al. (2013) Three centuries of shifting hydroclimatic regimes across the Mongolian Breadbasket. *Agric Meteorol* 178–179:10–20.
- Sternberg T (2010) Unravelling Mongolia's extreme winter disaster of 2010. *Nomad People* 14(1):72–86.
- Intergovernmental Panel on Climate Change (2007) *Climate Change 2007: The Physical Science Basis. Working Group I Contribution to the Fourth Assessment Report of the IPCC* (Cambridge University Press, Cambridge, UK).
- Graybill DA, Idso SB (1993) Detecting the aerial fertilization effect of atmospheric CO₂ enrichment in tree-ring chronologies. *Global Biogeochem Cycles* 7(1):81–95.
- Tucker C, Pinzon J, Brown M (2004) Global Inventory Modeling and Mapping Studies, NA94apr15b.n11-Vlg, 2.0 (Global Land Cover Facil, Univ of Md, College Park, MD). Available at <http://staff.glcf.umd.edu/sns/branch/htdocs/sns/data/gimms>.
- Cook ER, et al. (2013) Tree-ring reconstructed summer temperature anomalies for temperate East Asia since 800 C.E. *Clim Dyn* 41(11–12):2957–2972.

Supporting Information

Pederson et al. 10.1073/pnas.1318677111

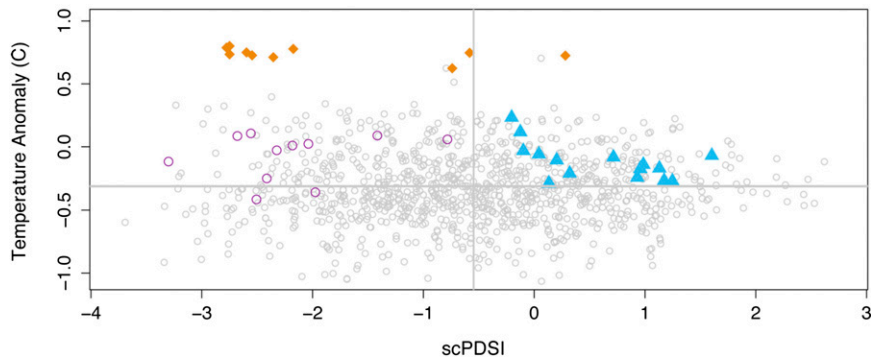


Fig. S1. Biplot of annual self-calibrated Palmer Drought Severity Index (scPDSI) (1) and reconstructed temperature anomalies (2) from 900 to 2009. Highlighted periods include 1180–1190 drought (magenta open circles), the Mongol Pluvial (blue triangles), and the 21st-century drought (orange diamonds).

1. Van der Schrier G, Barichivich J, Briffa KR, Jones PD (2013) A scPDSI-based global dataset of dry and wet spells for 1901–2009. *J Geophys Res Atmospheres* 118(10):4025–4048.
2. Cook ER, et al. (2013) Tree-ring reconstructed summer temperature anomalies for temperate East Asia since 800 C.E. *Clim Dyn* 41(11–12):2957–2972.

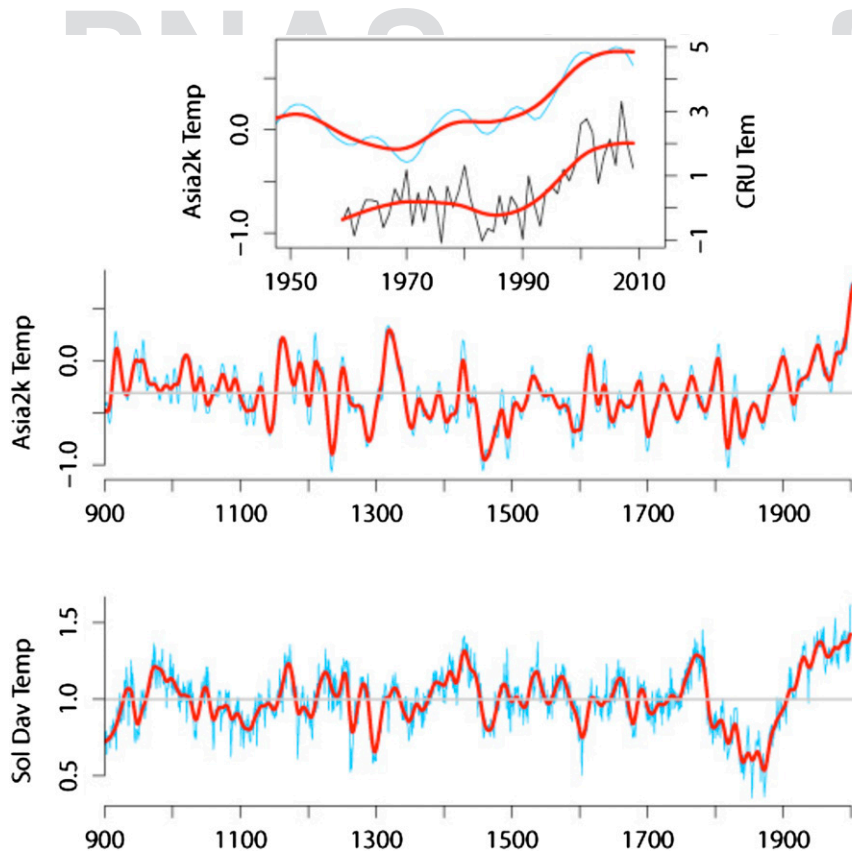


Fig. S2. Recent trends in summer temperature for central Mongolia (*Top*) based on Climatic Research Unit (CRU) land surface air temperature dataset version 4 (bounding box 48–52°N, 88–120°E) (black line) and reconstructed temperature in central Mongolia from 442 annual tree-ring chronologies (blue line) (*Middle*). Reconstructed temperature in central Mongolia (same as *Top*) here from 900 to 2009 CE and inferred temperature from one temperature-sensitive tree-ring site in central Mongolia (1) (*Bottom*). Red lines are 20-y splines.

1. Jones PD, et al. (2012) Hemispheric and large-scale land surface air temperature variations: An extensive revision and an update to 2010. *J Geophys Res*, 10.1029/2011JD017139.
2. Cook ER, et al. (2013) Tree-ring reconstructed summer temperature anomalies for temperate East Asia since 800 C.E. *Clim Dyn* 41(11–12):2957–2972.
3. D'Arrigo RD, et al. (2001) 1738 years of Mongolian temperature variability inferred from a tree-ring width chronology of Siberian pine. *Geophys Res Lett* 28(3):543–546.

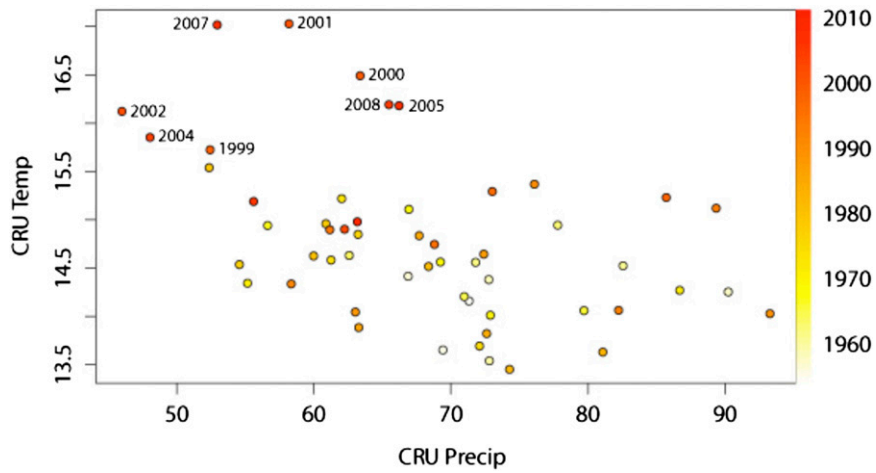


Fig. S3. Gridded growing season average monthly temperature [June, July, and August, CRU Time Series 3.10 0.5° (1)] and growing total season precipitation [June, July, August, and September, CRU TS 3.10.01 0.5° (1)] in north central Mongolia (bounding box 48–52°N, 88–120°E) with extreme temperatures of 1999–2008 labeled. Points are colored yellow to red by year.

1. Harris I, Jones PD, Osborn TJ, Lister DH (2013) Updated high-resolution grids of monthly climatic observations – the CRU TS3.10 Dataset. *Int J Climatol*, 10.1002/joc.3711.

PNAS proof
Embargoed

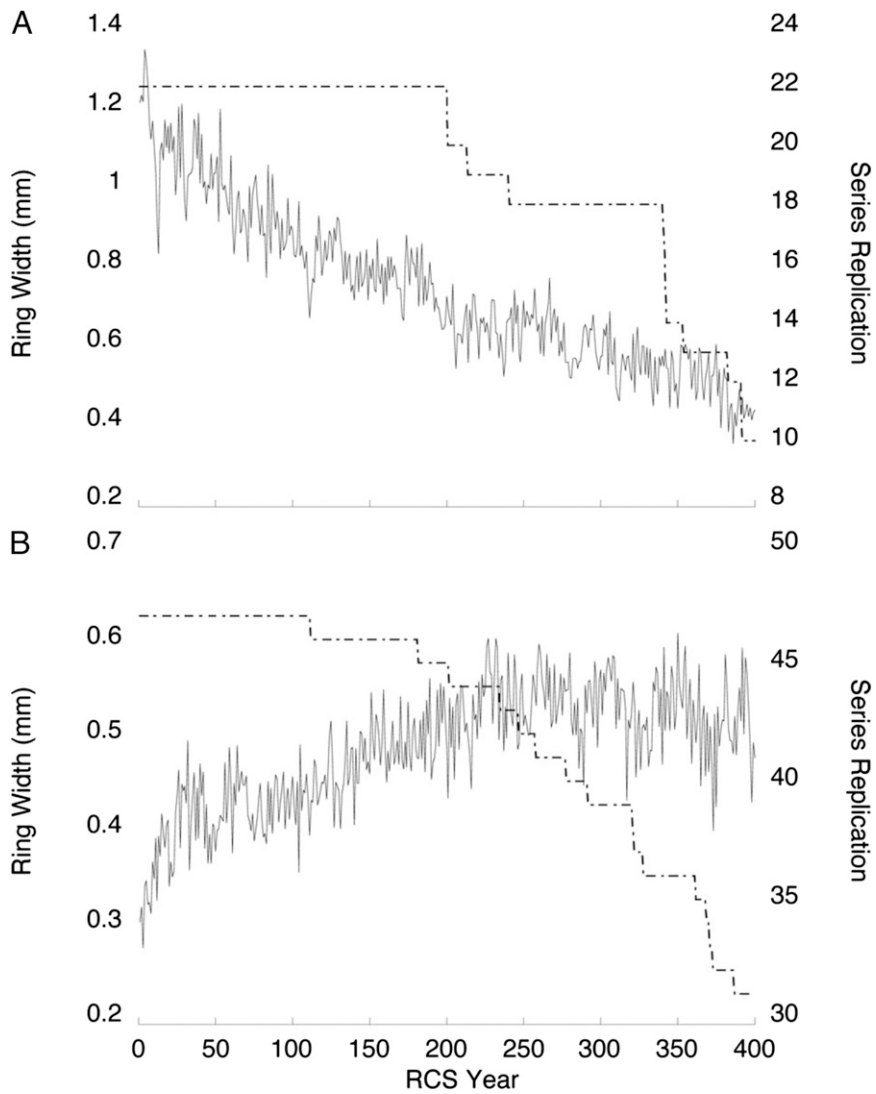


Fig. S4. Non strip-bark (with pith) (A) and strip-bark (B) regional curve standardization (RCS) curves. RCS aligns the inner ring date of all samples yielding typical radial growth patterns for a site, or in this case a subset of trees at a site. Ring index curves are the solid black lines, whereas the dashed black lines represent sample depth.

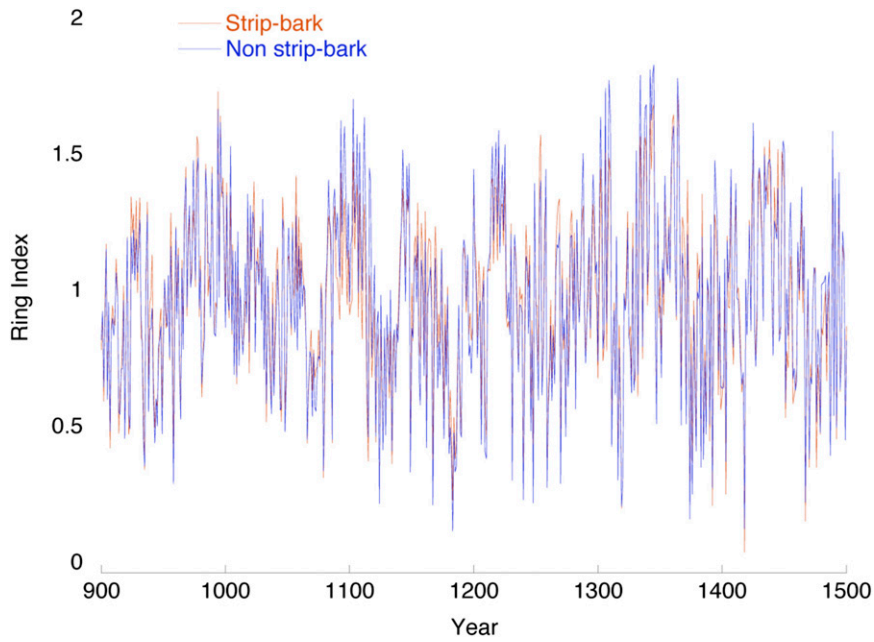


Fig. S5. Comparison of strip-bark (orange) and non strip-bark (blue) chronologies from 900 to 1500 CE, where sample depth for both portions of our total collection is relatively stable.

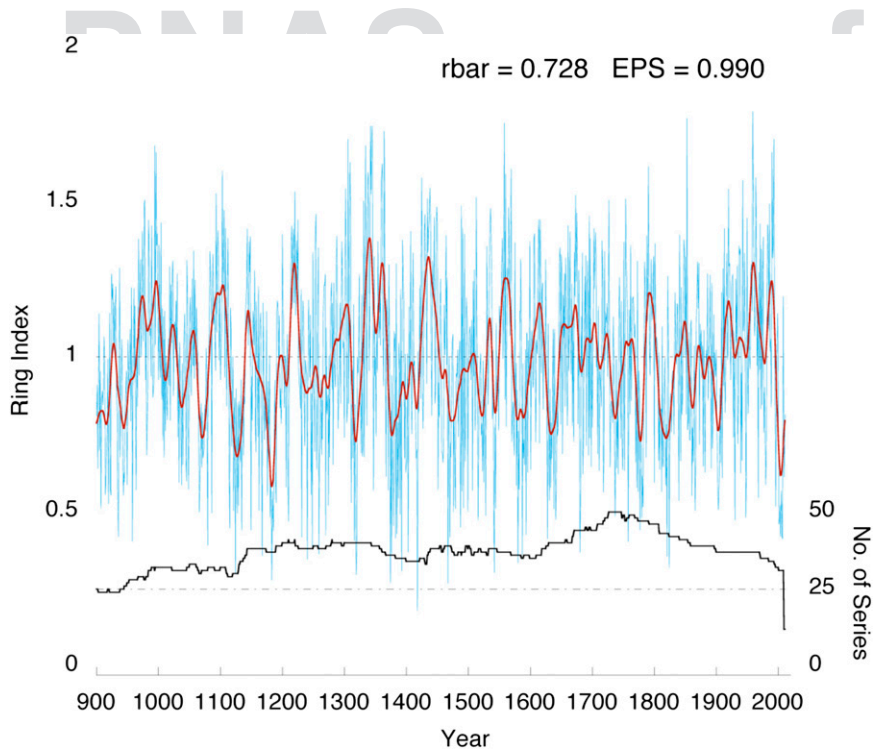


Fig. S6. Khorgo Lava pine chronology (*Top*): the blue curve is the annual record, the red curve is a 20-y spline of the annual record, and the mean is a horizontal dashed black line. Sample depth (*Bottom*) is the solid black curve. A sample depth of 25 series is represented by the black and horizontal dash-dotted line. Two measures of signal strength through time, expressed population signal (EPS) and the mean \bar{r} , are posted at the top right. Note the amount of white under the curve during the Mongol Pluvial of the early 1200s. It is the only pluvial since 900 CE with this structure, a structure lacking an annual value below the mean.

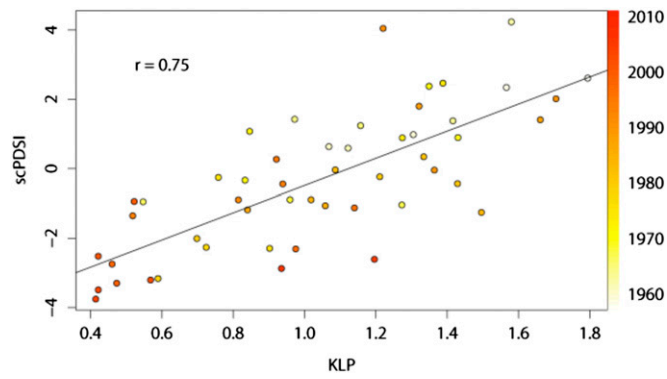


Fig. S7. Relationship between scPDSI (1) and tree-ring index 1959–2009.

1. Van der Schrier G, Barichivich J, Briffa KR, Jones PD (2013) A scPDSI-based global dataset of dry and wet spells for 1901–2009. *J Geophys Res Atmospheres* 118(10):4025–4048.

Table S1. Calibration–validation statistics for linear model predicting May–September scPDSI from the KLP tree-ring chronology

Calib.–Valid. Statistics	1959–1984		1985–2009		1959–2009
	Calib.	Valid.	Calib.	Valid.	Full period
Pearson r	0.755	0.701	0.755	0.701	0.747
RE	0.570	0.593	0.491	0.624	–
CE	0.570	0.361	0.491	0.362	–

Calib., calibration; CE, coefficient of efficiency; RE, reduction of error; Valid., validation. Durbin–Watson Stat = 1.1049.

PNAS proof
Embargoed